Meccanica (2012) 47:835–844
DOI 10.1007/s11012-011-9452-y

Dynamics of the shift in resonance frequency in a triple pendulum

Ivan Rivas-Cambero · Jose M. Sausedo-Solorio

Received: 31 July 2009 / Accepted: 15 June 2011 / Published online: 12 July 2011

Abstract We propose a general model for pendular systems with an arbitrary number of links arranged sequentially. The form of this model is easily adaptable to different settings and operating conditions. The main subject of analysis is a system obtained as a specific case taken from the general analysis, a three-links pendulum with damping subject to periodic perturbation. We performed a theoretical analysis of the frequency response and compared it with results from temporal integration. Moreover, a law was obtained explaining the behavior of the shift of the resonant frequencies due to a change in a parameter.

Keywords Triple pendulum · Resonance frequency · Frequency shift · Friction

1 Introduction

In general and whenever possible, at the starting point of any analysis of a system, a linear mathematical model is used. If the model is represented through differential equations, a further step is taken to propose a more detailed model, increasing the complexity of its equations and solution by using non-linear differential equations. Due to non-linearities in a system, some conditions might generate solutions with co-existing attractors or even chaotic behavior [1].

The interest in the study of pendular systems is continually increasing, based on the very rich dynamic behavior they display and the corresponding mathematical models that can be used to analyze very complex systems. Even a simple pendulum can be used as a standard benchmark to test another systems. Despite general models for an arbitrary number of links being used to control issues of the inverted pendulum [2], the lack of general models ready to apply to an n-links regular pendulum is well known. In [3] a model is proposed that uses equations of motion with a n-links pendulum fixed at its upper extremity using frictionless elements. Caertmell [4] developed a complete model of a plane pendulum for two links taking into account friction and compliance as well as links with variable lengths and masses.

Instead of using previously derived equations for a fixed number of links [5–8], we propose a general matrix representation for the n-links pendulum with damping. With this model, it is straightforward to decompose and separate the first derivatives of the dynamic variables as well as to solve the system equations using simulation language or a software package. Another kind of analysis tool is by means of a

I. Rivas-Cambero
División de Ingenierías, Universidad Politécnica de Tulancingo, Tulancingo Hidalgo, Mexico
e-mail: irivas@upt.edu.mx

J.M. Sausedo-Solorio (✉)
Centro de Investigación Avanzada en Ingeniería Industrial, Universidad Autónoma del Estado de Hidalgo, Pachuca Hidalgo, Mexico
e-mail: jmsaucedos@yahoo.com

symbolic system with a mathematical software package [9]. In [10], a scalable model of a mechanical system is used and the comparison between the dynamic simulation procedures is made per the proposal of this work. An interesting analysis is done in [11], where the authors found the chaotic dynamics of a triple pendulum controlled by a permanent rotating magneto and used Poincaré sections and graphs in phase space to analyze periodic and chaotic behaviors. Also, a non-linear model has been studied to compare the experimental results and calculations of a newly proposed non-linear model in the regime of transient chaos [12]. A study of a forced pendulum with non-linear torsion through bifurcation diagrams behaving as period doubling bifurcations to chaos is shown in [13]. Also in [14] experimental observations of chaos in a perturbed pendulum with damping with torque showing alternating behavior.

It is well known that behaviors in real systems are accompanied by both impact forces and friction [15]. Here, the authors model a physical plane triple pendulum with barriers causing impacts and sliding. Moreover, they investigate the stability of an orbit in perturbed dynamic systems and apply the results to a piston-connecting rod-crank in the one-cylinder of a combustion engine, in order to analyze the noise generated by the impacts between piston and cylinder. Several practical applications of multiple link pendulums have been done, such as the study of a triple pendulum used in the analysis of the swing of a golf club [16]. Here, the movement of a robot simulated for human tasks focused in the parameterization of optimal trajectories along time is analyzed. In addition, the decomposition of trajectories to characterize the way parameters influence behavior is shown.

Pendular systems have previously found application in the seismic isolation of vibration [17] where, as in this work, the modal frequency or response of the transference function is studied. Similarly, [18] presents analytical and experimental studies of a triple pendulum used as insulator of linear seismic movements with a non-linear viscosity and mechanisms for the dissipation of energy in bilinear hysteresis. Another application is a suspension system studied through different numerical models of a triple pendulum with the aim of filtering high frequencies of seismic noise [19]. In the same manner, in [20] a triple pendulum is used to suspend the optical system designed to diminish the effects of both seismic and thermal noise from the suspended masses of a laser interferometer geographic observatory (LIGO). And finally, an interesting optimization procedure can be found in [5], where the response of a triple pendulum from grouping parameters is tested to select the best approximation for a real system.

In this work the dynamic behavior of a plane triple pendulum is analyzed. A mathematical model with weightless-links from a Lagrange equations scheme is proposed. The model is written in matrix form, which is readily scalable to any number of links. Harmonic perturbation is applied to the upper link, leaving the remaining links free to oscillate. Every link is subjected to friction. Once the equations for an arbitrary number of links are obtained, the specific case for three links is analyzed and numerically solved. The frequency response regarding the friction parameter is obtained by finding a shift in the resonance peaks for every link. To verify the non-linear model, a simplified version for small oscillations is obtained and compared with other results [12–14] using reduced linear models for the triple pendulum. The structure of this work is as follows. In Sect. 2, the development of a nonlinear model in matrix from of a pendulum with three links with damping which is our main system is shown. This model was extracted from a general model of n-links developed in the Appendix. In Sect. 3, it is shown the dynamics of our system in a qualitative way. In Sect. 4, results of the frequency response are shown and compared with analytical calculations using an integral transform and the transference function. In Sect. 5 the main results of the work are shown, specifically, the shift of the frequency resonances and its relation to the friction parameter. Finally conclusions are presented in Sect. 6.

2 Mathematical model

In most published works on the triple pendulum, the specific model to be used is usually established in advance in terms of the equations of motion for the model in question. Here, we try to establish a general model for n-links and then deduce the specific case at hand. In the Appendix a general non-linear model for a plane pendulum with n-links and damping is developed. From there, the example of the triple pendulum system being analyzed is shown. The general non-linear model also provides the well-known small

oscillation model. In our system, each link is of negligible mass, but with a mass concentrated at the end of the link hanging from it, and its center of gravity coinciding with the axis of rotation from the adjoining link below. It is assumed that each joint is subject to friction opposing movement. A periodic disturbance[1] is applied to the top of the first link.

The schematic representation of this system is shown in Fig. 1. The masses and links length are labeled as m_i, and L_i, and the angles θ_i respectively ($i = 1, 2, 3$). The main dynamic variables are the angles θ_i measured from the vertical line to each link. The whole system is subjected to harmonic disturbance $\eta = \eta_0 \cos(\omega t)$ applied to the upper link.

The general model developed in the Appendix progresses toward writing the case for the triple pendulum. From Fig. 1, the dynamic variables are: $x_1 = L_1 \sin\theta_1$, $y_1 = -L_1 \cos\theta_1$, $x_2 = x_1 + L_2 \sin\theta_2$, $y_2 = y_1 - L_2 \cos\theta_2$, $x_3 = x_2 + L_3 \sin\theta_3$, and $y_3 = y_2 - L_3 \cos\theta_3$. Written equations (A.2) for three links, where the mathematical model depicted in matrix format is

$$M(\theta)\ddot{\theta} + N(\theta)\dot{\theta}^2 + R\dot{\theta} + P(\theta) + f(\theta, t) = 0 \qquad (1)$$

where

$$M(\theta) = \begin{bmatrix} M_1 & M_{12}\cos(\theta_1 - \theta_2) & M_{13}\cos(\theta_1 - \theta_3) \\ M_{12}\cos(\theta_1 - \theta_2) & M_2 & M_{23}\cos(\theta_2 - \theta_3) \\ M_{13}\cos(\theta_1 - \theta_3) & M_{23}\cos(\theta_2 - \theta_3) & M_3 \end{bmatrix},$$

$$N(\theta) = \begin{bmatrix} 0 & M_{12}\sin(\theta_1 - \theta_2) & M_{13}\sin(\theta_1 - \theta_3) \\ -M_{12}\sin(\theta_1 - \theta_2) & 0 & M_{23}\sin(\theta_2 - \theta_3) \\ -M_{13}\sin(\theta_1 - \theta_3) & -M_{23}\sin(\theta_2 - \theta_3) & 0 \end{bmatrix},$$

$$R = \begin{bmatrix} R_1 + R_2 & -R_2 & 0 \\ -R_2 & R_2 + R_3 & -R_3 \\ 0 & -R_3 & R_3 \end{bmatrix}, \quad P(\theta) = \begin{bmatrix} A_1 g \sin\theta_1 \\ A_2 g \sin\theta_2 \\ A_3 g \sin\theta_3 \end{bmatrix}, \quad f(\theta, t) = \begin{bmatrix} A_1 g \cos\theta_1 \\ A_2 g \cos\theta_2 \\ A_3 g \cos\theta_3 \end{bmatrix} \ddot{\eta},$$

the elements of the matrices are

$$M_1 = (m_1 + m_2 + m_3)L_1^2, \quad M_2 = (m_2 + m_3)L_2^2,$$
$$M_3 = m_3 L_3^2, \quad M_{12} = (m_2 + m_3)L_1 L_2,$$
$$M_{13} = m_3 L_1 L_3, \quad M_{23} = m_3 L_2 L_3,$$
$$A_1 = (m_1 + m_2 + m_3)L_1, \quad A_2 = (m_2 + m_3)L_2,$$
$$\text{and} \quad M_3 = m_3 L_3.$$

All other parameters are defined in the Appendix. These equations, of course, can be written as a system of three differential equations, too. But when contemplating the computational implementation, the matrix form is preferred.

3 Numerical solutions

The main model discussed in this work is the non-linear triple pendulum (i.e. large amplitudes of oscillation). It is widely known that the non-linear pendulum exhibits several regimes, such as periodic, quasi-periodic and chaotic. These characteristic behaviors are also obtained from our non-linear model. In Fig. 2, time series curves for θ_3 and the corresponding frequency response are shown. Curves in this figure are

[1] In this study, only periodic disturbance is considered. However, in future work other types of disturbances such as impulse and step functions will be used.

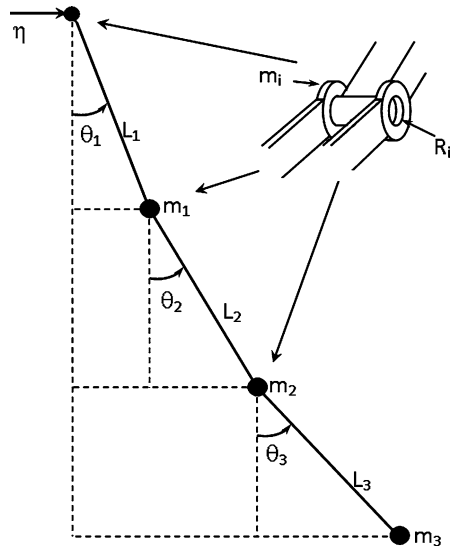

Fig. 1 Schematic representation of a triple pendulum with a perturbation in the upper link. The detail shows a joint among links consisting of a mass, and the damping mechanism

obtained by varying the perturbation frequency and the damping constant (in N m/s^2) to equal 1.0 for Fig. 2a, 0.1 for Fig. 2b, and 0.01 for Fig. 2c. In the same figure we can see the variation of the frequency components for each particular regime. Phase diagrams are used to visualize qualitatively a regime of movement. In Fig. 3 are drawn the corresponding phase diagrams for the cases of Figs. 2a, 2b, and 2c, they were obtained with the same parameters and initial conditions.

For small angles, the behavior of the small oscillations model (A.3), and the non-linear model in equations (1) tends to be the same as shown in Fig. 4. Both series will only coincide completely for $\sin\theta \approx \theta$, because it is fundamentally equivalent for considering the small oscillations model.[2] This figure shows a typical time series for the third angle for both models. One curve was obtained with the small oscillations model; the other with the non-linear model. Both curves were obtained for the same set of parameters and initial conditions. The values for perturbation frequency and amplitude perturbation are $f = 0.5$ Hz and $\eta = 0.03$ m, respectively. Masses and lengths have the same values $m_i = 1$ kg and $l_i = 1$ m $(i = 1, 2, 3)$ respectively.

[2]We have discovered a dependence of the system behavior on the friction parameter, although in this comparison we have not considered the friction term in obtaining time series. This should not be considered as validation of the proposed system. It is only the comparison within the limit of small oscillations.

4 Frequency response analysis

For the small oscillations model, we first calculate the theoretical solution of the frequency response using Transfer-Functions and then compare it with the numerical calculation using the corresponding differential equations (the solution of small oscillations). From (A.4) we get $ML\ddot{\theta} + R\dot{\theta} + gml\theta = -ml\ddot{\eta}$, and by applying the Laplace transform $MLs^2\theta(s) + Rs\theta(s) + gml\theta(s) = -mls^2\eta(s)$, and so $(MLs^2 + Rs + gml)\theta(s) = -mls^2\eta(s)$, where $\eta(s)$ and $\theta(s)$ are the input and the output variables respectively. A transfer function is defined as the rate of output to the input variable as

$$\frac{\theta(s)}{\eta(s)} = -\frac{mls^2}{MLs^2 + Rs + gml} \tag{2}$$

where s is a parameter. For this case, it is stated in (2) and displayed in Fig. 5a. In this figure, each peak corresponds to a resonance frequency of the system. Curve was obtained by using $s = j2\pi f$, and the same values used for Fig. 4. Figure 5b shows the frequency response for the small oscillations model in (A.4). It can be observed that the values for resonance frequencies are the same obtained through using both methods.

Figure 5c shows the behavior of frequency response using the differential equations of the non-linear model for the triple pendulum. This diagram was obtained with the same values for parameters as Fig. 5a and Fig. 5b. Although the first peak is the same for three cases, for $f > 0.35$ Hz resonance peaks widen. This happens because non-linearity starts to influence pendulum behavior by degrading the response to perturbation frequency.

With the results represented in Fig. 5, it is possible to compare the frequency of resonance calculated with the transfer function $G(s)$, with the frequency response for $\theta_3(t)$ calculated from the differential equations of the small oscillation model, and with the non-linear model. We should not make a comparison of peak heights in this figure, in Fig. 5a they correspond to a ratio of transfer but in Figs. 5b and 5c, to the angle of oscillation of a particular link from the physical system.

Figures 5b and 5c correspond to the heights of the peaks observed in the third link for each frequency of disturbance. This can be seen as the response to the frequency being disturbed of the small oscillations

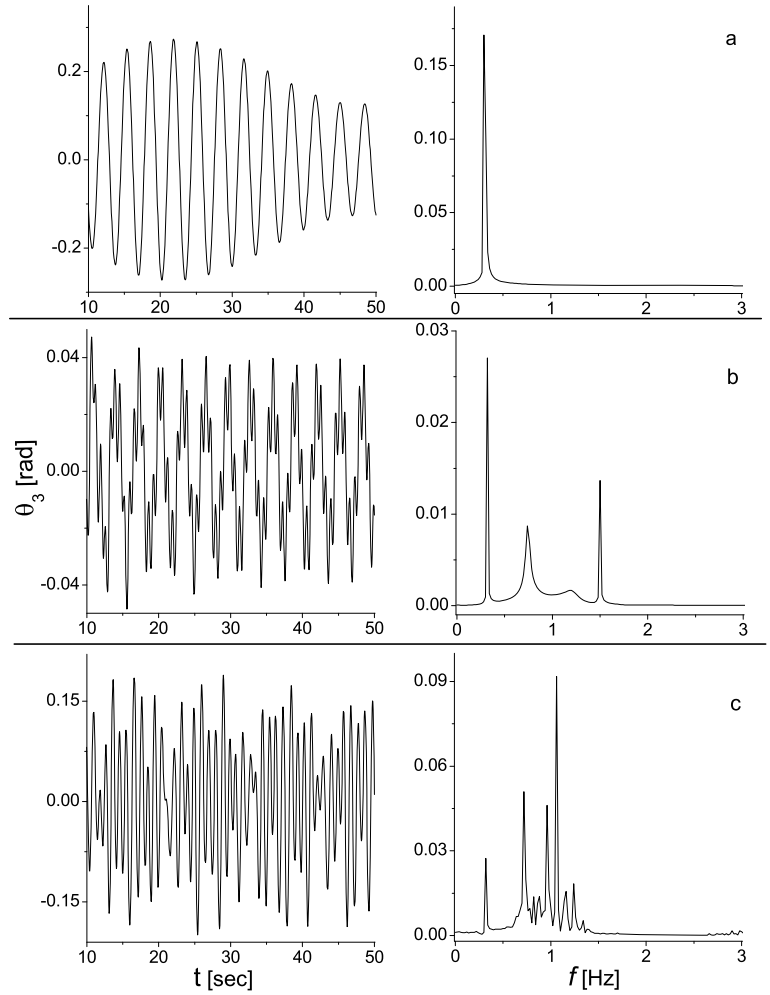

Fig. 2 Time series curves for and the corresponding frequency spectrum for different regimes typical of the pendulum obtained by varying the perturbation frequency and damping are shown. For the third angle θ_3, we have: (**a**) Periodic motion with $f = 0.3$ Hz, and damping of 1 N m/s^2, (**b**) Quasi-periodic motion with $f = 1.5$ Hz, damping of 0.1 N m/s^2 and (**c**) Chaotic behavior with $f = 0.5$ Hz, damping of 0.01 N m/s^2. Graphs of spectral analysis are shown on the *right*

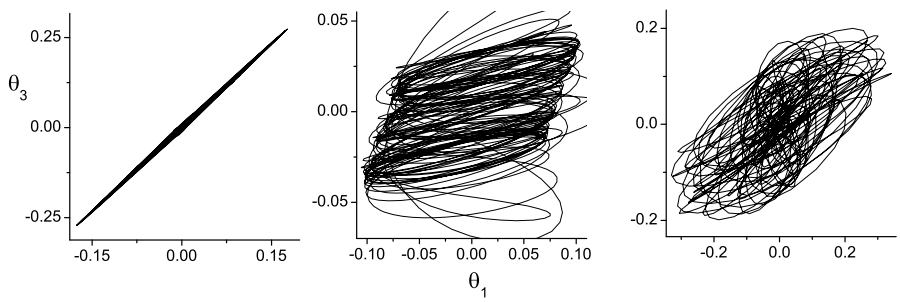

Fig. 3 Phase diagrams for variable θ_3 vs. θ_1 calculated with same parameters as for Fig. 2. Every plot (**a**), (**b**), and (**c**) correspond to plots 2(a), 2(b), and 2(c) respectively

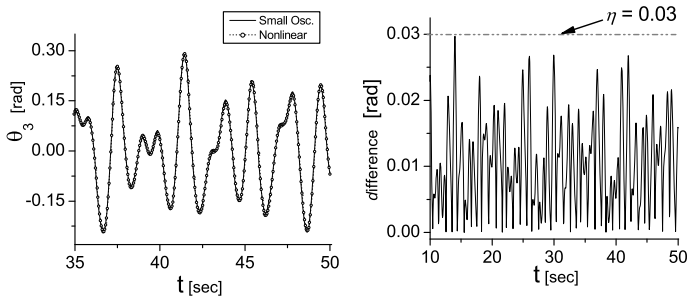

Fig. 4 Comparison between response of the small oscillations and nonlinear models. (**a**) Time series for the angle of the third link, with perturbation frequency $f = 0.5$ Hz. Both curves were obtained with the same parameters and initial conditions. (**b**) Difference between the two time series. The maximum value of the difference is function of the disturbance amplitude η which in this case has a value of 0.03

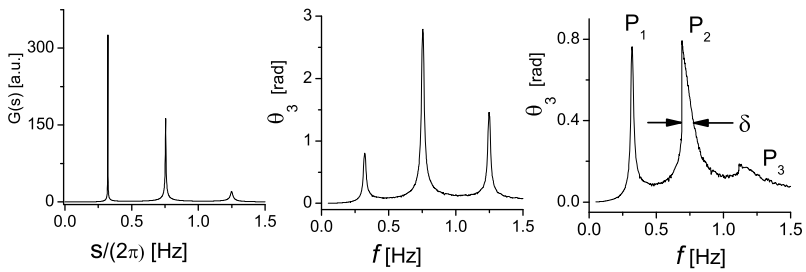

Fig. 5 Resonance frequencies of the linear triple pendulum model for the angle of the last link (θ_3) as a function of the perturbation frequency. Frequency response diagrams using (**a**) theoretical Laplace Transform, (**b**) the small oscillations model solution, and (**c**) the non-linear model

model (A.4) and the non-linear model (A.2). It can be noted that as we move away from the first link the width of the peak grows. This indicates that the lower elements of the pendulum respond to an increasingly wider range of frequencies.

Figure 6 shows how the width of the peaks changes as a function of the position of each link in Fig. 5c. As we move from the first to the last link, the width of the peak grows. Thus, the effect caused by the non-linearity in the pendulum model is a degradation of its theoretical resonant frequencies.

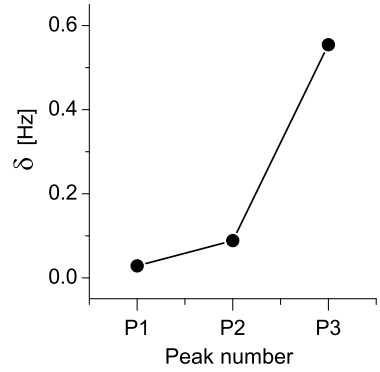

Fig. 6 Change of width of the three peaks in Fig. 5c for the third link of pendulum. The increase of the width can be seen as a degradation of the resonant frequencies caused by non-linearity

5 Shift in resonance frequency

A study of the dynamic properties of the triple pendulum with the damping varying in each joint was performed. First, in analyzing the behavior of the system around the frequency resonance peaks, a slow exponential decaying in the maximum amplitude of angles has been found, as the friction coefficient increase. This is shown in Fig. 7, where vertical axes in a log scale correspond to the maximum angle reached for every link and horizontal axes correspond to the variation of the friction coefficient, remaining the same for all links ranging from 0 to 1 N m/s^2. It has been discovered that according to (3) these curves have

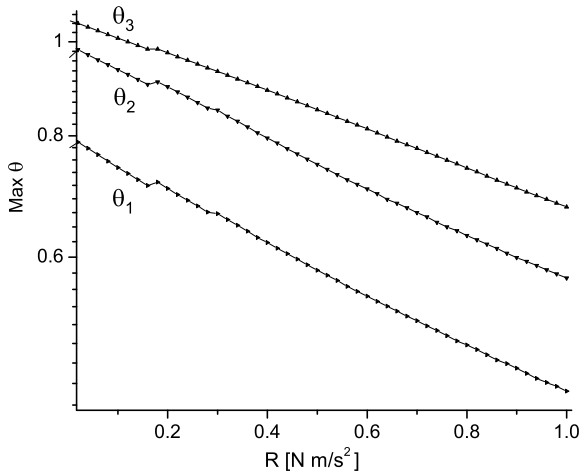

Fig. 7 Maximum values in steady state for each angle using a frequency equal to the first resonance peak. The *vertical axis* scale is logarithmic

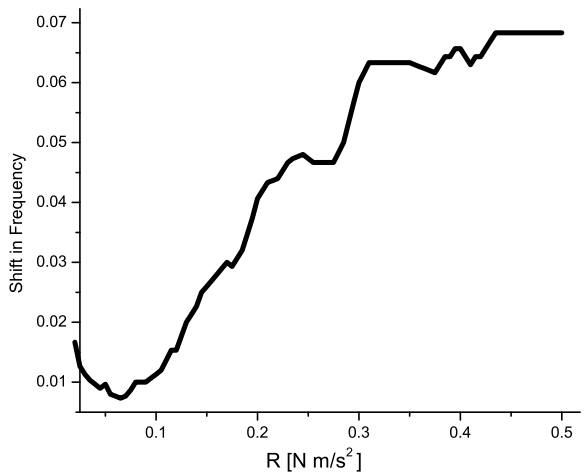

Fig. 8 Shift of the second resonance frequency peak. Two different behaviors can be seen: one where friction does not influence the peak in frequency and another where the shift grows linearly with the damping parameter

an exponential decay with a scaling law of approximately 0.50:

$$\theta_{max} \sim e^{-0.5R} \tag{3}$$

In addition, the main result of this work has been the finding that resonance frequencies shift with changes in friction. The behavior of this shift for the second resonance frequency peak is shown in Fig. 8 for the third angle of the system, where the range of frequency value was varied from 0.63 to 0.75 Hz and the friction constant ranged from 0 to 0.5 N m/s^2 to encompass every curve.

Two different behaviors have been found when the friction varies in the joints. First, where the shift is independent for small values of the friction parameter, meaning $R_k < 0.1$, the friction does not displace the peaks of resonance with the same behavior that occurs when $R_k > 0.3$. Second, on the half of the interval with values for R_k ranging from 0.1 to 0.3, the linear behavior obtained signifies that the shift in resonance peaks grows linearly as friction with a slope of 0.25 i.e. $\Delta f_r = 0.25R$.

6 Conclusions

For a non-linear model based on the Lagrangian formulation obtained for a pendulum with n-links, it has been proven that its applicability and simplicity of use is based on the representation stated in this work. From the representation with second order differential equations, the matrix representation has been proposed in terms of first derivatives of the dynamic variables, however separate from them. Such representation has a direct implementation in a computational language or software package, so a program model for a pendulum with an arbitrary number of links can be written directly. The main system analyzed was obtained as a specific case of the general multi-link version. This case for three links is in full agreement with the corresponding models published elsewhere.

Our non-linear model was proved against a small oscillations version by calculating frequency response, time series, and spectral analysis and obtaining similar dynamic behavior in the limit case. In the analysis made for the frequency response, three different strategies were used to compare peaks of resonance: one by means of the small oscillations model, another by using transfer functions based on the Laplace transform, and the third by our non-linear model. The comparison of the position of the peaks of resonance in each case was almost exact. But one of the main results obtained was in the analysis of the shift of frequency resonances. Two distinct behaviors have been observed: one where friction in the joints does not affect frequencies; the other resulting in the scaling law determining the behavior of the resonance shifts.

Having laws governing the behavior of a system is critical in the design of a structure or mechanism. The

results from this work provide a method for analyzing how the resonance frequency peaks behave when there are changing parameters for the system. The fact that the lowest elements of the pendulum respond to a broader spectrum of frequencies must be taken into account when designing compensation mechanisms of movement caused by earthquakes in large buildings. This is due to the counterweights used to follow the dynamics of multi-link pendulums. One way to control unwanted oscillations in this system is achieved by using a brake mechanism at each joint. This is capable of altering the natural frequency as demonstrated in this research.

Appendix

Obtaining small oscillations model from the nonlinear model. In order to establish the system discussed herein, we start from a general mathematical approach to an n-links pendulum. Then we deduce the main model used here.

The mathematical model for a multi-link pendulum can be built based on the Euler-Lagrange formulation [21],

$$\frac{d}{dt}\frac{\partial L}{\partial \dot{\theta}_k} - \frac{\partial L}{\partial \theta_k} + \frac{\partial Q}{\partial \dot{\theta}_k} = 0 \tag{A.1}$$

where $L = T - u$ is the Lagrangian, $T = \frac{1}{2}\Sigma m_k |r_k \dot{\theta}_k|^2$, $u = g\Sigma m_k h_k$, $Q = \frac{1}{2}\Sigma R_k(\dot{\theta}_k - \dot{\theta}_{k-1})^2$ are the friction losses, and θ_k represents the generalized coordinates. After replacing these terms in (A.1), we can establish a non-linear differential equations system, written in a matrix form for a pendulum with an arbitrary number of links as:

$$M_N(\theta)\ddot{\theta}_N + N_N(\theta)\dot{\theta}_N^2 + R_N\dot{\theta}_N + P_N(\theta) + f_N(\theta, t) = 0 \tag{A.2}$$

where M_N, N_N, R_N and f_N are matrices given by:

$$M_N(\theta) = \begin{bmatrix} M_1 & M_{12}\cos(\theta_1-\theta_2) & M_{13}\cos(\theta_1-\theta_3) & \cdots & M_{1n}\cos(\theta_1-\theta_n) \\ M_{12}\cos(\theta_1-\theta_2) & M_2 & M_{23}\cos(\theta_2-\theta_3) & \cdots & M_{2n}\cos(\theta_2-\theta_n) \\ M_{13}\cos(\theta_1-\theta_3) & M_{23}\cos(\theta_2-\theta_3) & M_3 & \cdots & M_{3n}\cos(\theta_3-\theta_n) \\ \vdots & \vdots & \vdots & \ddots & \vdots \\ M_{1n}\cos(\theta_1-\theta_n) & M_{2n}\cos(\theta_2-\theta_n) & M_{3n}\cos(\theta_3-\theta_n) & \cdots & M_n \end{bmatrix}$$

$$N_N(\theta) = \begin{bmatrix} 0 & M_{12}\sin(\theta_1-\theta_2) & M_{13}\sin(\theta_1-\theta_3) & \cdots & M_{1n}\sin(\theta_1-\theta_n) \\ -M_{12}\sin(\theta_1-\theta_2) & 0 & M_{23}\sin(\theta_2-\theta_3) & \cdots & M_{2n}\sin(\theta_2-\theta_n) \\ -M_{13}\sin(\theta_1-\theta_3) & -M_{23}\sin(\theta_2-\theta_3) & 0 & \cdots & M_{3n}\sin(\theta_3-\theta_n) \\ \vdots & \vdots & \vdots & \ddots & \vdots \\ -M_{1n}\sin(\theta_1-\theta_n) & -M_{2n}\sin(\theta_2-\theta_n) & -M_{3n}\sin(\theta_3-\theta_n) & \cdots & 0 \end{bmatrix}$$

$$R_N = \begin{bmatrix} R_1+R_2 & -R_2 & 0 & \cdots & 0 \\ -R_2 & R_2+R_3 & -R_3 & \cdots & 0 \\ 0 & -R_3 & R_3+R_4 & \cdots & 0 \\ \vdots & \vdots & \vdots & \ddots & \vdots \\ 0 & 0 & 0 & \cdots & R_n \end{bmatrix}, \quad P_N(\theta) = \begin{bmatrix} A_1 g\sin\theta_1 \\ A_2 g\sin\theta_2 \\ A_3 g\sin\theta_3 \\ \vdots \\ A_n g\sin\theta_n \end{bmatrix}, \quad f_N(\theta,t) = \begin{bmatrix} A_1 g\cos\theta_1 \\ A_2 g\cos\theta_2 \\ A_3 g\cos\theta_3 \\ \vdots \\ A_n g\cos\theta_n \end{bmatrix}\ddot{\eta},$$

and

$$\ddot{\theta}_N = \begin{bmatrix} \ddot{\theta}_1 \\ \ddot{\theta}_2 \\ \ddot{\theta}_3 \\ \vdots \\ \ddot{\theta}_n \end{bmatrix}, \qquad \dot{\theta}_N = \begin{bmatrix} \dot{\theta}_1 \\ \dot{\theta}_2 \\ \dot{\theta}_3 \\ \vdots \\ \dot{\theta}_n \end{bmatrix}, \qquad \theta_N = \begin{bmatrix} \theta_1 \\ \theta_2 \\ \theta_3 \\ \vdots \\ \theta_n \end{bmatrix}.$$

From this model, it is straightforward to obtain the case of small oscillations (i.e when $\sin\theta \approx \theta$). Thus resulting in n-links pendular systems with small oscillations. For the small oscillations model of a pendulum we have:

$$M_N L_N \ddot{\theta}_N + R_N \dot{\theta}_N + g m_n l_N \theta_N + m_N l_N \eta_{Na} = 0 \tag{A.3}$$

where:

$$M_N = \begin{bmatrix} m_1 L_1 & m_2 L_1 & m_3 L_1 & \cdots & m_n L_1 \\ 0 & m_2 L_2 & m_3 L_2 & \cdots & m_n L_2 \\ 0 & 0 & m_3 L_3 & \cdots & m_n L_3 \\ \vdots & \vdots & \vdots & \ddots & \vdots \\ 0 & 0 & 0 & \cdots & m_n L_n \end{bmatrix},$$

$$L_N = \begin{bmatrix} L_1 & 0 & 0 & \cdots & 0 \\ L_1 & L_2 & 0 & \cdots & 0 \\ L_1 & L_2 & L_3 & \cdots & 0 \\ \vdots & \vdots & \vdots & \ddots & \vdots \\ L_1 & L_2 & L_3 & \cdots & L_n \end{bmatrix},$$

$$R_N = \begin{bmatrix} R_1 + R_2 & -R_2 & 0 & \cdots & 0 \\ -R_2 & R_2 + R_3 & -R_3 & \cdots & 0 \\ 0 & -R_3 & R_3 + R_4 & \cdots & 0 \\ \vdots & \vdots & \vdots & \ddots & \vdots \\ 0 & 0 & 0 & \cdots & R_n \end{bmatrix},$$

$$l_N = \begin{bmatrix} L_1 & 0 & 0 & \cdots & 0 \\ 0 & L_2 & 0 & \cdots & 0 \\ 0 & 0 & L_3 & \cdots & 0 \\ \vdots & \vdots & \vdots & \ddots & \vdots \\ 0 & 0 & 0 & \cdots & L_n \end{bmatrix},$$

$$m_N = \begin{bmatrix} m_1 + m_2 + m_3 + \cdots + m_n & 0 & 0 & \cdots & 0 \\ 0 & m_2 + m_3 + \cdots + m_n & 0 & \cdots & 0 \\ 0 & 0 & m_3 + \cdots + m_n & \cdots & 0 \\ \vdots & \vdots & \vdots & \ddots & \vdots \\ 0 & 0 & 0 & \cdots & m_n \end{bmatrix}, \qquad \eta_{Na} = \begin{bmatrix} \ddot{\eta} \\ \ddot{\eta} \\ \ddot{\eta} \\ \vdots \\ \ddot{\eta} \end{bmatrix}.$$

A specific case concerns the 3-links pendulum subject to small-oscillations. From (A.3), we deduce:

$$ML\ddot{\theta} + R\dot{\theta} + gml\theta + ml\eta_a = 0 \tag{A.4}$$

with

$$M = \begin{bmatrix} m_1 L_1 & m_2 L_1 & m_3 L_1 \\ 0 & m_2 L_2 & m_3 L_2 \\ 0 & 0 & m_3 L_3 \end{bmatrix},$$

$$L = \begin{bmatrix} L_1 & 0 & 0 \\ L_1 & L_2 & 0 \\ L_1 & L_2 & L_3 \end{bmatrix},$$

$$R = \begin{bmatrix} R_1 + R_2 & -R_2 & 0 \\ -R_2 & R_2 + R_3 & -R_3 \\ 0 & -R_3 & R_3 \end{bmatrix},$$

$$l_N = \begin{bmatrix} L_1 & 0 & 0 \\ 0 & L_2 & 0 \\ 0 & 0 & L_3 \end{bmatrix},$$

$$m = \begin{bmatrix} m_1 + m_2 + m_3 & 0 & 0 \\ 0 & m_2 + m_3 + & 0 \\ 0 & 0 & m_3 \end{bmatrix},$$

$$\ddot{\theta} = \begin{bmatrix} \ddot{\theta}_1 \\ \ddot{\theta}_2 \\ \ddot{\theta}_3 \end{bmatrix}, \qquad \dot{\theta} = \begin{bmatrix} \dot{\theta}_1 \\ \dot{\theta}_2 \\ \dot{\theta}_3 \end{bmatrix}, \qquad \theta = \begin{bmatrix} \theta_1 \\ \theta_2 \\ \theta_3 \end{bmatrix},$$

$$\eta_a = \begin{bmatrix} \ddot{\eta} \\ \ddot{\eta} \\ \ddot{\eta} \end{bmatrix}.$$

This is in complete agreement with the well-known small oscillations model appearing elsewhere [21].

Computational implementation. Given the second-order differential equations that describe the pendulum model of n-links, for the purpose of computational implementation, the model is transformed into a system of equations of the first order with the first derivatives already separated as described by:

$$d\theta = M_a(\theta)^{-1}[-N_a(\theta)v_a - P_a(\theta) - f_a(\theta, t)] \tag{A.5}$$

where $d\theta = [\dot{u}\ \dot{v}\ \dot{w}\ \dot{\theta}_1\ \dot{\theta}_2\ \dot{\theta}_3]^T$,
$v_a = [u^2\ v^2\ w^2\ -u\ -v\ -w]^T$, and the 6×6 partitioned matrix defined as

$$M_a(\theta) = \begin{bmatrix} M(\theta) & R \\ 0 & I \end{bmatrix}, \qquad N_a(\theta) = \begin{bmatrix} N(\theta) & 0 \\ 0 & I \end{bmatrix},$$

$$P_a(\theta) = \begin{bmatrix} P(\theta) \\ 0 \end{bmatrix}, \qquad f_a(\theta, t) = \begin{bmatrix} f(\theta, t) \\ 0 \end{bmatrix}, \quad \text{and}$$

$$I = \begin{bmatrix} 1 & 0 & 0 \\ 0 & 1 & 0 \\ 0 & 0 & 1 \end{bmatrix}.$$

Matrices $M(\theta)$, $N(\theta)$, $P(\theta)$, and $f(\theta, t)$ was defined in (1).

References

1. Sado D, Gajos K (2003) Note on chaos in three degree of freedom dynamical system with double pendulum. Meccanica 38:719–729
2. Lobas L (2007) The equations of an inverted pendulum with an arbitrary number of links and an asymmetric follower force. Int Appl Mech 43(5):106–114
3. Campbell S, Chancelier J, Nikoukhah R (2006) Modeling and simulation in scilab/scicos. Springer, New York, Chap 5
4. Caertmell M (2003) On the need for control of nonlinear oscillations in machine systems. Meccanica 38:185–212
5. Awrejcewicz J, Kudra G (2008) Dynamics of a real triple pendulum-modeling and experimental observation. In: ENOC, Saint Petersburg, Russia
6. Awrejcewicz J, Kudra G, Wasilewsky G (2007) Experimental and numerical investigation of chaotic regions in the physical pendulum. Nonlinear Dyn 50:755–766
7. Kim D, Singhose W (2006) Reduction of double-pendulum bridge crane oscillations. In: 8th Int conf on motion and vib ctl
8. Husman M, Torrie C, Plissi M, Robertson N, Strain K, Hough J (2000) Modeling of multi-stage pendulums: Triple pendulum suspension for GEO 600, Rev. Sci. Instr 71(6)
9. Gmiterko A, Grossman M (2010) Nlink inverted pendulum modeling. In: Recent advances in mechatronics 2008–2009, part 3. Springer, Berlin, pp 151–156
10. Schmitt A, Bender J (2005) Impulse based dynamic simulation of multibody systems: numerical comparison with standard methods. In: Proc. automation of discrete production engineering, pp 324–329
11. Berdahl J, Vander L (2001) Magnetically driven chaotic pendulum. Am J Phys 69(9):1016–1019
12. Sousa de Paula A, Amorin M, Lunes F (2006) Chaos and transient in an experimental nonlinear pendulum. J Sound Vib 294(3):585–595
13. Beckert S, Schock U, Schulz C, Weidlich T, Kaiser F (1987) Experiments on the bifurcation behavior of a forced nonlinear pendulum. Phys Lett A 107:347–350
14. Blackburn J, Yang Z, Vik S (1987) Experimental study of chaos in a driven pendulum. Physica D 26:385–395
15. Awrejcewicz J, Kudra G, Lamarque C (2003) Dynamics investigation of three couple rods with a horizontal barrier. Meccanica 38:687–698
16. Aicardi M (2007) A triple pendulum robotic model and a set of simple parametric functions for the analysis of the golf swing. Int J Sport Sci Eng 1(2):75–86
17. Wu W (2007) Instrumentation of the next generation gravitational wave detector: Triple pendulum suspension and electro-optic modulator. PhD Dissertation, University of Florida, USA
18. Morgan T (2007) The use of innovative base isolation systems to achieve complex seismic performance objective. PhD Dissertation, University of California, Berkeley, USA
19. Ruet L (2007) Active control and sensor noise filtering duality application to advanced LIGO suspension. PhD Dissertation. Ins. Nat. Sci. App. de Lyon
20. Plissi M, Torrie C, Barton M, Robertson N (2004) An investigation of eddy-current damping of multistage pendulum suspensions for use in interferometric gravitational wave detector. Rev Sci Instrum 75(11):4516–4522
21. Golstein H, Poole C, Safko J (2003) Classical mechanics, 3rd edn. Addison Wesley, New York